Strong magnetoelectric coupling in multiferroic $BiFeO_3$–$Pb(Zr_{0.52}Ti_{0.48})O_3$ composite films derived from electrophoretic deposition

Yujie Wu, Jian-guo Wan,[a] Chuanfu Huang, Yuyan Weng, Shifeng Zhao, Jun-ming Liu, and Guanghou Wang

Department of Physics and National Laboratory of Solid State Microstructures, Nanjing University, Nanjing 210093, People's Republic of China and International Center for Materials Physics, Chinese Academy of Sciences, Shenyang 110016, People's Republic of China

(Received 27 June 2008; accepted 28 October 2008; published online 14 November 2008)

The $BiFeO_3$–$Pb(Zr_{0.52}Ti_{0.48})O_3$ composite film in which $BiFeO_3$ nanoparticles are distributed in the $Pb(Zr_{0.52}Ti_{0.48})O_3$ matrix was prepared by electrophoretic deposition method. The microstructural characterization revealed the structural distortion of the $BiFeO_3$ phase, induced by the unique $BiFeO_3$–$Pb(Zr_{0.52}Ti_{0.48})O_3$ core/shell structure. The composite film exhibited evidence of ferroelectricity with enhanced ferromagnetism as well as a magnetoelectric effect. The two origins for the magnetoelectric effect are presented. This present work provides a promising roadmap to improve the magnetoelectric effect of $BiFeO_3$-based multiferroics for actual applications. © *2008 American Institute of Physics*. [DOI: 10.1063/1.3028089]

In the past few decades, there has been an increasing interest in multiferroic materials due to their attractive physical properties and potential applications in sensors, data storage devices, transducers, etc.[1] Up to date, many multiferroic compounds such as Cr_2O_3, $YMnO_3$, $TbMnO_3$, etc. have been found.[2–4] Unfortunately, for most of them the magnetoelectric effect at room temperature is too small to be utilized for practical purpose.

Recently, the multiferroic $BiFeO_3$ compound (BFO) (with perovskite ABO_3 structure) has been drawing much attention because it exhibits both ferroelectricity and antiferromagnetism above room temperature. However, the room-temperature magnetoelectric effect in pure BFO is still weak due to its weak magnetism and ferroelectricity as well as high leakage current. Many attempts have been made to solve these problems. For example, in order to reduce the leakage current or enhance the ferroelectricity of BFO, several approaches, including the preparation of solid solution with other ferroelectric materials (e.g., $BaTiO_3$)[5] and the fabrication of *A*-site-ion-doped BFO compounds (e.g., $Bi_{1-x}Sm_xFeO_3$, $Bi_{1-x}La_xFeO_3$),[6,7] have been developed. On the other hand, based on the structure modulation, some routes have been developed to enhance the magnetism of BFO, including the preparation of epitaxial BFO films[8] and *B*-site-ion-doped BFO compounds (e.g.,$BiFe_{1-x}Mn_xO_3$, $BiFe_{1-x-y}Co_xNb_yO_3$).[9,10] In spite of these, up to now there are few reports on enhancement of both ferroelectric polarization and magnetization in BFO-based materials, which is important for strong magnetoelectric coupling.

In this letter, we report the achievement of simultaneous enhancement of ferroelectricity and ferromagnetism in a core-shell BFO–$Pb(Zr_{0.52}Ti_{0.48})O_3$ (PZT) composite film. Due to the introduction of highly insulating PZT with good ferroelectricity, the ferroelectricity and insulating property of the composite film can be improved. Meanwhile, the good interfacial coupling between BFO and PZT will lead to the structure distortion of BFO, which significantly enhances the magnetization of BFO. Therefore, strong magnetoelectric coupling in such composite film can be expected.

We developed an effective method, namely, electrophoretic deposition technique, to prepare the BFO-PZT composite film. First, the BFO particles with average diameter of ~50 nm were synthesized via sol-gel method and then dispersed into 2-methoxyethanol solution in which polyvinylpyrrolidone (PVP) (K-30) was added to control the viscosity for the formation of the stable suspension solution. During the electrophoretic deposition, two platinum plates were used as the cathode and anode. A $Pt/Ti/SiO_2/Si$ wafer was chosen as the substrate, which was clamped on the cathode. The applied voltage between the electrodes was 350 V. The electrophoretic deposition lasted 5 min. After that, the substrate with deposited BFO particles was dried in air for 5 min at 280 °C. Scanning electron microscopy (SEM) (LEO-1530VP) revealed that most BFO particles were discretely distributed on the substrate surface [shown in inset (a) of Fig. 1]. Subsequently, based on the sol-gel process, two-layer PZT gel films were spin coated onto the substrate with BFO particles to form the composite film. Finally, the composite film was annealed at 650 °C in a rapid annealing oven for 5

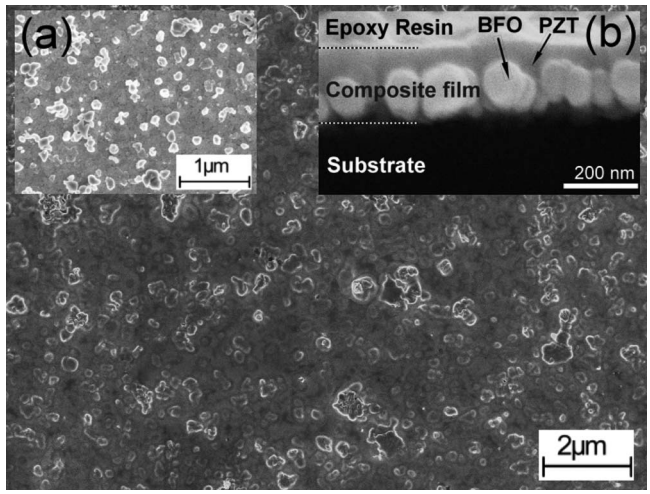

FIG. 1. SEM image of the BFO-PZT composite film. Inset (a) is the SEM image of the BFO particles on the substrate deposited by electrophoretic deposition process and inset (b) is the cross-section SEM image of the composite film.

[a]Author to whom correspondence should be addressed. Electronic mail: wanjg@nju.edu.cn.

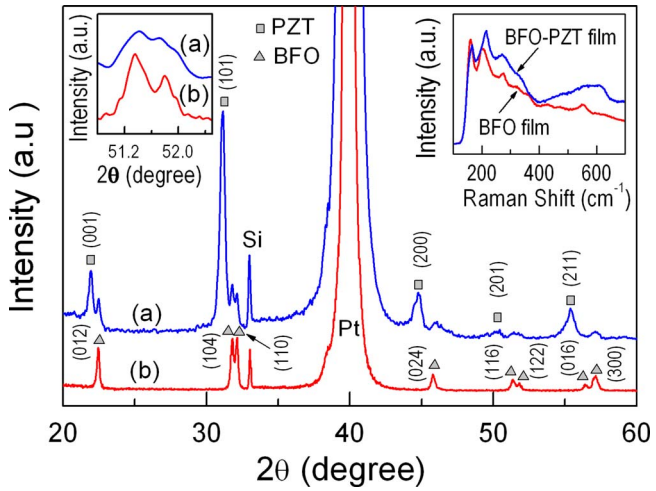

FIG. 2. (Color online) XRD patterns of the (a) BFO-PZT composite film and (b) pure BFO film. The left inset is the magnified XRD patterns in the vicinity of $2\theta=51°$ and the right inset is the Raman spectra of the films.

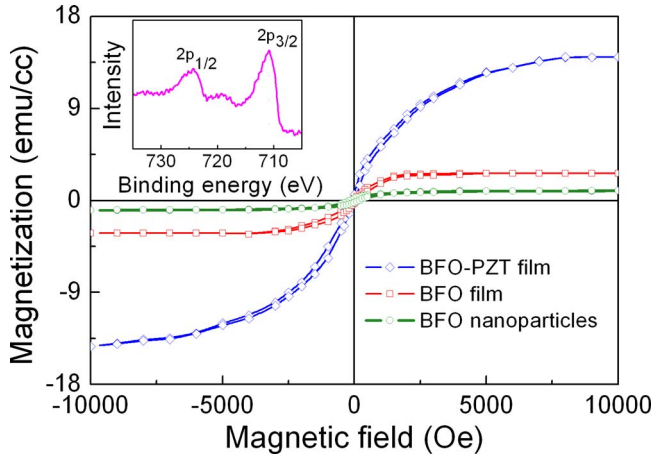

FIG. 3. (Color online) Magnetic hysteresis loop measured at room temperature for the (a) BFO-PZT composite film, (b) pure BFO film, and (c) BFO nanoparticles. Inset is the XPS spectrum of the composite film.

min under the oxygen atmosphere with O_2 flow of 2 L/min. The final film thickness is $t\sim200$ nm.

The surface and cross-section SEM images of the composite film were then examined, as shown in Fig. 1. The composite film exhibits the mixed connective types. That is, the film consists of the upper PZT thin layer and the bottom composite layer (2–2 type) and in the bottom layer the BFO particles are uniformly distributed in the PZT matrix (0–3 type). The volume fraction of the BFO particles in the composite film, which is calculated using the energy dispersive x-ray spectrum, is ~0.22. In addition, one observes that each BFO particle is closely wrapped by an outer PZT layer and a core/shell structure is formed. The formation of such core/shell structure should be attributed to the PVP, which acts as a soft template to induce the nucleation and growth of the PZT layer on the surface of BFO particles.[11]

In each core/shell structure, since there exists the lattice mismatch between BFO and PZT (PZT has tetragonal structure with $a=b=4.036$ Å and $c=4.146$ Å, while BFO is of rhombohedral structure with $a=b=c=5.63$ Å), a stress inside BFO particles will be generated, which results in the crystal lattice distortion of BFO. In order to confirm this, we analyzed the x-ray diffraction (XRD) spectrum of the film, as shown in Fig. 2, spectrum (a). Two evident sets of diffraction peaks were observed. Apart from these reflections from BFO and PZT, there exist no additional or intermediate phase peaks. In addition, from the magnified patterns in the vicinity of $2\theta=51°$ (shown in the left inset of Fig. 2), two neighboring BFO diffraction peaks of (116) and (122) tend to merge into a single broad peak [Contrastively, in the pure BFO film prepared by a sol-gel process, these two peaks are clearly separate, as shown in Fig. 2, spectrum (b)]. This indicates that the structure of BFO in the composite film is significantly distorted, giving rise to the transition from the rhombohedral structure to tetragonal one.[12] Furthermore, we performed the microarea Raman spectra analysis (Ntegra Spectra Nanolaboratory, NT-MDT Co.) on the samples. The data are presented in the right inset of Fig. 2. For pure BFO film, the Raman peaks at ~160 and ~200 cm^{-1}, respectively, correspond to the $A_1(2TO)$ and $A_1(3TO)$ phonon modes associated with the Bi–O bond. Comparatively, for the BFO-PZT composite film, the corresponding peaks have an evident redshift and broadening, which implies that there exists internal stress in the BFO phase.[13]

Figure 3(a) presents the field dependent in-plane magnetization of the composite film measured at room temperature by a superconducting quantum interference device magnetometer. The composite film exhibits evident ferromagnetic characteristic (The out-plane magnetization loop is almost the same as the in-plane one, not shown here). The saturation magnetization is as high as $M_s\sim14$ emu/cc, much larger than that of the BFO film [~3 emu/cc, as shown in Fig. 3(b)] and the BFO nanoparticles [~1 emu/cc, as shown in Fig. 3(c)]. According to previous investigations, the ferromagnetism enhancement in our composite film may be attributed to two reasons. One is the formation of Fe^{2+} ions in BFO,[14] and the other is the internal stress in BFO.[8] In order to examine whether there are Fe^{2+} ions in our composite film, we further performed the x-ray photoemission spectroscopy (XPS) measurement, as shown in inset of Fig. 3. It is well known that Fe $2p$ core level splits into $2p_{1/2}$ and $2p_{3/2}$ components. The binding energy of Fe $2p_{3/2}$ is expected to be 710.7 eV for the Fe^{3+} while 709.3 eV for the Fe^{2+}. From the XPS spectrum, we observe that the peak of Fe $2p_{3/2}$ is exactly located at 710.8 eV. Moreover, its satellite peak is closer to the side of the Fe $2p_{1/2}$ peak. These two characteristics indicate that the Fe valence in the composite film should be Fe^{3+} and there is no Fe^{2+} ions.[15] Accordingly, we confirm that the ferromagnetism enhancement in the composite film should be mainly caused by the internal stress in BFO.

For the ferroelectric measurement, Au electrodes with diameter of 0.2 mm were deposited onto the film surface. Figure 4 presents the ferroelectric polarization of the composite film as function of electric field measured by a RT-66A ferroelectric measuring unit. The measurement frequency is 500 Hz and the applied voltage is in the range of 2–10 V. The composite film exhibits evidence of ferroelectricity. The remanent polarization reaches $2P_r=39$ $\mu C/cm^2$ at 50 MV/m, which is better than that of pure BFO ceramics and most BFO films,[16,17] and comparable to those ion-doped BFO films.[6,7] We notice that at high electric field the ferroelectric loop of the film somewhat shows the rounded characteristic of leakage. In order to understand this further, we subsequently carried out the steady-state leakage current measurement, as shown in the upper inset of Fig. 4. The

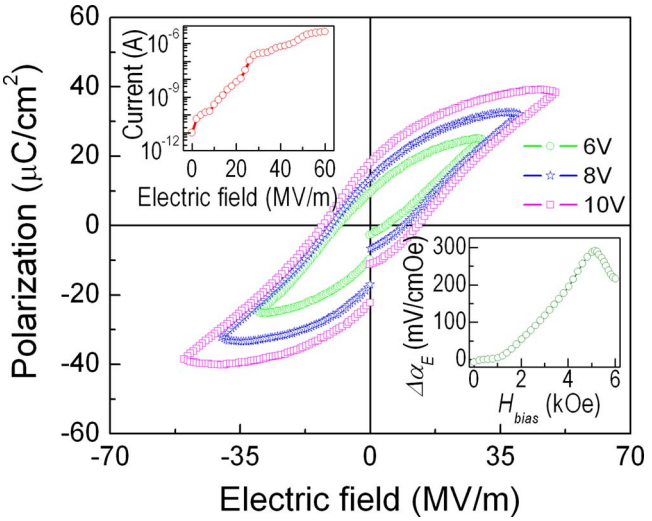

FIG. 4. (Color online) Polarization as function of electric field in the BFO-PZT composite film. Upper inset is the leakage current as function of electric field. Bottom inset is the variation in the increment in α_E with H_{bias} measured at $f=1$ kHz.

voltage was stepped at 20 mV/step with duty cycle of 100% and integrate time of 320 ms. It is seen that the leakage current in the film is $\sim 2.7\times 10^{-6}$ A at 50 MV/m. In spite of this, the leakage under low electric field is too small to be ignored, which does not influence the magnetoelectric effect.

We finally measured the magnetoelectric effect of the composite film. A small alternating magnetic field H (5 Oe, generated by a pair of Helmholtz coils) together with a parallel magnetic bias H_{bias} (generated by an electromagnet) were applied along the film plane. The induced voltage V was measured using a lock-in amplifier (SRS Inc., SR830). During the measurement, the system was well electric-shielded and the interfering signal caused by the electromagnetic induction of the system was carefully eliminated. The magnetoelectric effect was characterized by the magnetoelectric voltage coefficient $\alpha_E = d(V/t)/dH$. The bottom inset of Fig. 4 presents the increment in $\alpha_E(\Delta\alpha_E)$ as function of H_{bias} at fixed alternating magnetic frequency $f=1$ kHz. A strong magnetoelectric coupling in the composite film was observed. The $\Delta\alpha_E$ value increases with the increasing H_{bias} until it reaches the maximum at $H_{\text{bias}}\sim 5.1$ kOe, and then drops. The maximum $\Delta\alpha_E$ value is as high as ~ 300 mV/cm Oe, much larger than previously reported values in the other BFO-based materials.[18,19]

We then discuss the origin of magnetoelectric effect in the composite film. First and importantly, BFO plays a key role in the magnetoelectric coupling process. Some previous investigations revealed that in an analogous multiferroic compound any reversal of the ferroelectric order parameter was accompanied by a simultaneous reversal of the magnetic order parameter.[20] In detail, the spontaneous electric polarization in BFO is directed along the [111] axes, while the preferred orientation of the magnetic moments is in the (111) plane.[21] Thus it is expected that the ferroelectric switching leads to the reorientation of the ferromagnetic order, consequently leading to a magnetoelectric coupling in BFO. Another non-negligible origin should be attributed to the product property, namely, the magnetomechanical-electric transformation through the stress-mediated transfer on the interface between the ferromagnetism of BFO and ferroelectricity of PZT.[11] We notice that our composite film is composed of enormous number of core/shell BFO-PZT particles. Although these particles are randomly aligned along various orientations, each core/shell structure is well-defined with good interface, which is even analogous to a heteroepitaxial structure. Therefore, the interaction between BFO and PZT in each core/shell particle is greatly efficient, consequently results in the strong magnetoelectric coupling in whole composite film. We believe that the above two magnetoelectric coupling processes as well as their cooperative effect are all crucial for the magnetoelectric effect in the composite film.

In summary, the core/shell BFO-PZT composite film was prepared by electrophoretic deposition technique combined with sol-gel process. Due to the unique core/shell structure, the composite film exhibits evidence of ferroelectricity with enhanced ferromagnetism as well as a magnetoelectric effect. The two origins, namely, direct coupling between ferroelectric and ferromagnetic orders in BFO and ferroelectric-ferromagnetic coupling between BFO and PZT, are responsible for the magnetoelectric effect in the composite film.

This work was supported by the National Natural Science Foundation of China (Grant Nos. 10774070 and 90606002), the Provincial Nature Science Foundation of Jiangsu in China (Grant Nos. BK2006123 and BK2008024), the National Key Projects for Basic Research of China (Grant No. 2009CB623300), and the Program for New Century Excellent Talents in University of China (Grant No. NCET-07-0422).

[1] N. A. Spaldin and M. Fiebig, Science **309**, 391 (2005).
[2] M. Muto, Y. Tanabe, T. Lizuka-Sakano, and E. Hanamura, Phys. Rev. B **57**, 9586 (1998).
[3] M. Fiebig, T. Lottermoser, D. Frohlich, A. V. Goitsev, and R. V. Pisarev, Nature (London) **419**, 818 (2002).
[4] T. Kimura, T. Goto, H. Shinatani, K. Ishizaka, T. Arima, and Y. Tokura, Nature (London) **426**, 55 (2003).
[5] M. M. Kumar, A. Srinivas, and S. V. Suryanarayana, J. Appl. Phys. **87**, 855 (2000).
[6] G. L. Yuan and S. W. Or, J. Appl. Phys. **100**, 024109 (2006).
[7] D. Lee, M. G. Kim, S. Ryu, H. M. Jang, and S. G. Lee, Appl. Phys. Lett. **86**, 222903 (2005).
[8] J. Wang, J. B. Neaton, H. Zheng, V. Nagarajan, S. B. Ogale, B. Liu, D. Viehland, V. Vaithyanathan, D. G. Schlom, U. V. Waghmare, N. A. Spaldin, K. M. Rabe, M. Wuttig, and R. Ramesh, Science **299**, 1719 (2003).
[9] M. Azuma, H. Kanda, A. A. Belik, Y. Shimakawa, and M. Takano, J. Magn. Magn. Mater. **310**, 1177 (2007).
[10] Y. K. Jun and S. H. Hong, Solid State Commun. **144**, 329 (2007).
[11] J. G. Wan, H. Zhang, X. W. Wang, D. Y. Pan, J.-M. Liu, and G. H. Wang, Appl. Phys. Lett. **89**, 122914 (2006).
[12] Z. X. Cheng, A. H. Li, X. L. Wang, S. X. Dou, K. Ozawa, H. Kimura, S. J. Zhang, and T. R. Shrout, J. Appl. Phys. **103**, 07E507 (2008).
[13] F. Q. Song, M. Han, M. D. Liu, B. Chen, J. G. Wan, and G. H. Wang, Phys. Rev. Lett. **94**, 093401 (2005).
[14] W. Eerenstein, F. D. Morrison, J. Dho, M. G. Blamire, J. F. Scott, and N. D. Mathur, Science **307**, 1203a (2005).
[15] P. C. J. Graat and M. A. J. Somers, Appl. Surf. Sci. **100**, 36 (1996).
[16] V. R. Palkar, J. John, and R. Pinto, Appl. Phys. Lett. **80**, 1628 (2002).
[17] Y. P. Wang, L. Zhou, M. F. Zhang, X. Y. Chen, J.-M. Liu, and Z. G. Liu, Appl. Phys. Lett. **84**, 1731 (2004).
[18] Q. H. Jiang, J. Ma, Y. H. Lin, C. W. Nan, Z. Shi, and Z. J. Shen, Appl. Phys. Lett. **91**, 022914 (2007).
[19] J. M. Caicedo, J. A. Zapata, M. E. Gómez, and P. Prieto, J. Appl. Phys. **103**, 07E306 (2008).
[20] T. Zhao, A. Scholl, F. Zavaliche, K. Lee, M. Barry, A. Doran, M. P. Cruz, Y. H. Chu, C. Ederer, N. A. Spaldin, R. R. Das, D. M. Kim, S. H. Baek, C. B. Eom, and R. Ramesh, Nature Mater. **5**, 823 (2006).
[21] C. Ederer and N. A. Spaldin, Phys. Rev. B **71**, 060401(R) (2005).